PCCP

Accepted Manuscript

ROYAL SOCIETY OF CHEMISTRY

www.rsc.org/pccp

Concentration effects on spontaneous and amplified emission in benzo[c]fluorenes

Karolis Kazlauskas [a,*], Gediminas Kreiza [a], Edvinas Radiunas [a], Povilas Adomėnas [a], Ona Adomėnienė [a], Karolis Karpavičius [a], Jonas Bucevičius [b], Vygintas Jankauskas [c], Saulius Juršėnas [a]

[a] *Institute of Applied Research, Vilnius University, Saulėtekio 9-III, LT-10222 Vilnius, Lithuania*

[b] *Department of Organic Chemistry, Faculty of Chemistry, Vilnius University, Naugarduko 24, LT-03225 Vilnius, Lithuania*

[c] *Department of Solid State Electronics, Vilnius University, Saulėtekio 9-III, LT-10222 Vilnius, Lithuania*

* Corresponding author. Tel.: +370 5 2366032; fax: +370 5 2366059.
E-mail address: karolis.kazlauskas@ff.vu.lt (K. Kazlauskas).

Abstract

Deep-blue-emitting benzo[c]fluorene-cored compounds featuring twisted peripheral moieties for suppressed concentration quenching of emission were synthesized and investigated as potential materials for light amplification. The detailed study of concentration effects on the spontaneous and stimulated emission, excited-state lifetime and susceptibility to aggregate formation carried out for different benzofluorenes enabled to understand the concentration dependence of amplified spontaneous emission (ASE) threshold and to reveal the optimal concentration for the lowest threshold. The weak concentration quenching accompanied by high fluorescence quantum yield (>40 %) and radiative decay rate (>5×10^8 s^{-1}) enabled to attain the lowest ASE threshold in the neat amorphous film of benzofluorene bearing dihexylfluorenyl peripheral moieties. Aggregate formation was found to negligibly affect emission efficiency of the benzofluorene films, however it drastically increased ASE threshold *via* enhanced scattering of directional stimulated emission, and thereby implied necessity to utilize homogeneous glassy films as the lasing media. Although the bulky dihexylfluorenyl groups at periphery ensured formation of glassy benzofluorene films with the ASE threshold as low as 900 W/cm^2 (under nanosecond excitation), they adversely affected carrier drift mobility implying a tradeoff between ASE and charge transport properties for the lasing

materials utilized in the neat form. Such low ASE threshold attained in air is among the lowest reported for solution-processed neat films. The low threshold and enhanced photostability of benzofluorenes against fluorene compounds in air show great potential for benzofluorene-cored molecular glasses as active media for lasing applications.

Keywords: amplified spontaneous emission; fluorene; fluorescence; drift mobility; laser

1. Introduction

Strong interest in laser sources based on low-cost organic semiconductors is provoked by their attractive electronic and optical properties combined with the mechanical flexibility and ease of processibility.[1,2] Indeed, simple fabrication of optoelectronic devices *via s*olution processing (*e.g.* ink-jet printing) is one of the key advantages of organic semiconductors.[3,4] Even vacuum evaporation of amorphous organic films is much less demanding than epitaxial growth of inorganic crystals.[5] Furthermore, organic lasers can be potentially compact and ready for integration with other optoelectronic devices since amorphous films permit deposition on a variety of substrates. Broad gain spectra accompanied by the numerous choice of organic lasing materials offer wide emission-wavelength tunability across the entire visible range.[1] Another great advantage of organic lasers is negligible temperature dependence of stimulated emission threshold, output power and emission wavelength, which is a result of molecular origin of the electronic transitions, *i.e.*, strongly localized excited states (excitons), involved in light emission.[5,6] These features make organic laser sources relevant to applications in spectroscopy as well as optical data communications, memory, sensing and displays.[5,7]

Although the breakthrough in material and device design have enabled to reduce lasing thresholds down to a few watts per square centimeter in the optically-pumped state-of-the-art DFB polymer lasers,[8] great challenges still remain in attaining organic lasers with direct electrical pumping.[1,2] Some of the main issues relate to self-absorption losses, low carrier mobility, polaron absorption, quenching by electrodes and poor photostability of organic compounds.[1,2,5–7,9–11] The poor stability substantially shortens the lifetime of organic lasers making it unacceptable for practical applications.[1] This can be justified by insufficiently low amplified spontaneous emission (ASE) threshold causing to use pumps at high fluences and thereby facilitating faster degradation of organic materials. Meanwhile, the minimization of self-absorption losses is essential for obtaining high optical gain, since a low absorbance at the emission wavelength entails reduced pump threshold for population inversion. From this point of view disordered organic semiconductors are highly beneficial, because the presence of a significant Stokes shift enables moving of emission wavelength to a spectral region where absorptive losses are smaller.[11] Sometimes energy-transfer mechanism is employed for larger energetic separation of absorption and emission by making guest-host blends,[12] however in this case, the redshifted emission can be more readily quenched due to polaron absorption.

The issue of low carrier mobility makes it hard to reach sufficiently high current densities corresponding to threshold exciton concentrations. Low mobility causes high concentration of

polarons especially near the contacts subsequently inducing charge quenching (due to polaron absorption) and quenching from the electrodes.[5] In addition to charge quenching, singlet exciton annihilation is identified as another major loss mechanism.[1,13] Importantly, both loss mechanisms are mediated by intermolecular (or inter-chain) coupling,[1] which is known to be sensitive to packing morphology of the solid films and to their preparation conditions.[11] Typically, at high concentrations or in the solid state intermolecular interactions are enhanced leading to the formation of poorly emissive aggregate or excimer species.[14] Hence, a straightforward way to preserve high emission efficiency and low stimulated emission threshold is to reduce intermolecular coupling by increasing the distance between neighboring molecules. The control of intermolecular interactions was attempted via different approaches, *e.g.,* blending with a host material, incorporating bulky side groups, utilizing dendritic or spiro compounds.[5] Unfortunately, realization of efficient laser requires high chromophore density[1] and high carrier mobility, *i.e*, a features that are barely consistent with a necessity to decrease intermolecular coupling. This imposes a certain tradeoff in the properties of lasing materials and also points out the importance of developing new compounds featuring not only low ASE threshold, but also weak concentration quenching of emission and high carrier mobility.

To this end, a series of low-molecular-weight compounds utilizing benzo[c]fluorene core and bulky peripheral groups for prevention of concentration quenching were synthesized and investigated as potential lasing materials. The fluorene moieties, frequently used as the main building blocks for construction of organic lasers, were employed for their superior emission efficiency, large radiative decay rate, and thus, for high likelihood of low ASE threshold.[5,15–17] To enhance conjugation and rigidity of the compounds, the fluorene was fused with an additional benzene ring (so as to form benzo[c]fluorene) and used as the core, whereas to ensure weak concentration quenching the twisted molecular geometries resulting from sterically hindered aromatic peripheral moieties decorated with branched alkyl chains (in some of the compounds) were employed. Benzofluorene derivatives were previously utilized in light-emitting devices as hosts or dopants mainly in spiro configuration,[18–20] however no data on the ASE properties of the compounds was reported yet. For comparison purposes, a similar fluorene-cored compound was studied as the reference. The suitability of the benzo[c]fluorenes for light amplification was assessed by evaluating concentration quenching of spontaneous and amplified emission, by establishing relationship between pump thresholds of ASE and compound concentration as well as by quantifying radiative decay rates, photostability and carrier drift mobility.

2. Experimental

2.1. Materials

The details on the starting materials, intermediates as well as the target benzo[c]fluorenes **BF8**, **BF9**, **BF12** and the reference compound **BF14** are provided in the Supplementary Information.

2.2. Instrumentation

H^1, C^{13} NMR spectra were measured using Varian UNITY INOVA 300 (300 MHz) and BRUKER ASCEND 400 (400 MHz) spectrometers for compounds (6)-(8) and (13)-(15), respectively. Purity of the synthesized materials was analyzed using Agilent Technologies 6890N Network GC System and Agilent Technologies 7890C GC systems gas chromatographs. Mass spectra were set using Agilent Technologies 5975C gas chromatograph/mass selective detector (GC/MSD) system with the triple-axis detector. HRMS mass spectrometry were carried out on a quadrupole, time-of-flight mass spectrometer (micrOTOF-Q II, Bruker Daltonik GmbH). Differential scanning calorimetry (DSC) measurements were carried out using thermal analysis system DSC 8500 (Perkin Elmer) at a heating/cooling rate of 10 °C/min under nitrogen flow. Optical properties of the compounds were assessed in dilute 10^{-5} M tetrahydrofuran (THF) solutions and neat films prepared from 10^{-2} M THF solutions. Due to the poor solubility of compound BF9 in THF, solvent chlorobenzene was used instead. The neat films were obtained by spin-coating THF solutions of the studied compounds on pre-cleaned glass substrates. Absorption spectra were recorded on a UV−Vis−NIR spectrophotometer Lambda 950 (Perkin-Elmer). Fluorescence of the investigated compounds was excited by a Xe lamp coupled to the monochromator (FWHM<10 meV) and measured using a back-thinned CCD spectrometer PMA-11 (Hamamatsu). Excitation wavelength was close to the absorption band maximum of compounds. Fluorescence transients were measured at fluorescence band maximum using a time-correlated single photon counting system PicoHarp 300 (PicoQuant), which utilized a semiconductor diode laser (repetition rate 1 MHz, pulse duration 70 ps, emission wavelength 370 nm) as an excitation source. Fluorescence quantum yields (Φ_F) of the solutions were estimated using the integrated sphere method.[21] An integrating sphere (Sphere Optics) coupled to the CCD spectrometer via optical fiber was also employed to measure Φ_F of the films. Concentration quenching of emission was evaluated by dispersing molecules in an inert polymer polystyrene (PS) matrix and estimating Φ_F dynamics *vs* molecule concentration in the range of 0.5 – 100 wt %. The PS films with dispersed compounds were prepared by dissolving the compounds

and PS at appropriate ratios in toluene solutions and then casting the solutions on pre-clean glass substrates. Phosphorescence spectra of the compounds dispersed in PS at a concentration of 1.0 wt % were measured in a closed-cycle helium cryostat at 20 K temperature by utilizing the time-gated intensified CCD camera iStar (Andor). Amplified spontaneous emission (ASE) measurements were carried out by exciting the films with a 40-μm-wide laser stripe focused on the film surface near its freshly cleaved edge by using a cylindrical lens (the so-called thin excitation stripe geometry).[22,23] Wavelength-tunable optical parametric amplifier (EKSPLA) pumped by nanosecond Nd^{3+}:YAG laser (pulse duration 5 ns, repetition rate 10 Hz) was used to excite the films at the absorption band maximum. Excitation power density in the ASE measurements was varied by several orders of magnitude from 0.3 to 1800 kW/cm^2 to determine the ASE threshold. The same pulsed excitation source was employed to test the photostability of the studied compounds. Optical microscopy images of the films in the dark field were obtained using microscope BX51 (Olympus). Morphology of the films was assessed by atomic force microscopy (Witec alpha300 S). Carrier drift mobility of the wet-casted neat films with the thickness of 3−6 μm was measured by xerographic time-of-flight (XTOF) method.[24,25] The samples for the charge carrier mobility measurements were prepared as described elsewhere.[26,27]

3. Results and discussion

3.1. Synthesis of benzo[c]fluorene derivatives

Synthesis of 5,9-diaryl-7,7-dimethyl-7H-benzo[c]fluorenes was carried out according to the Scheme 1.

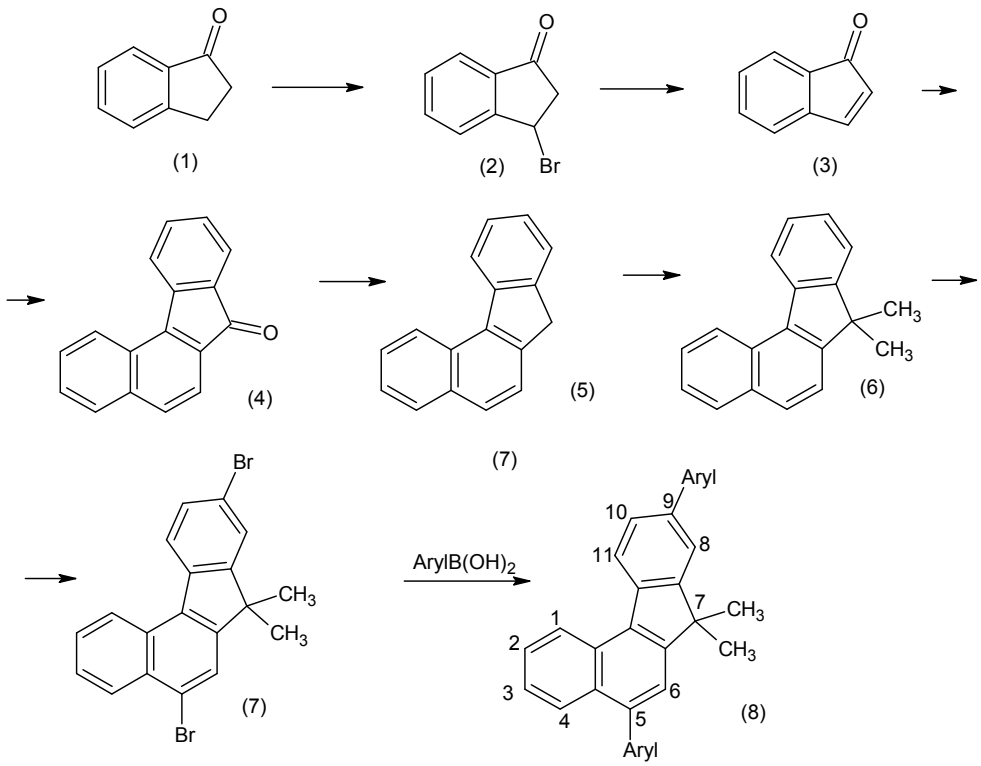

Here

Aryl	Product (8)
4-Ethoxyphenyl-	**BF8** 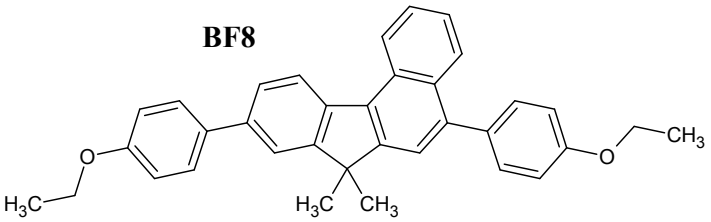
4-Biphenylyl-	**BF9** 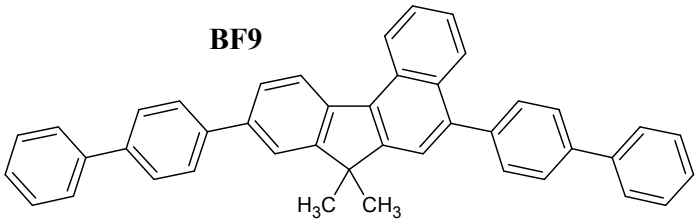
9,9-Dihexyl-9H-fluoren-3-yl-	**BF12** 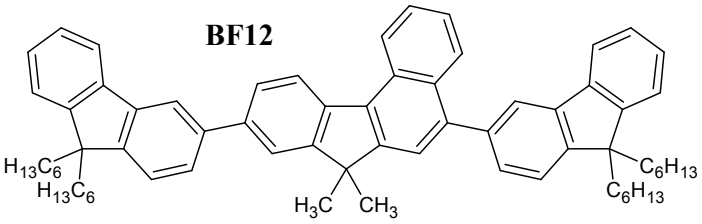

Scheme 1 Synthesis route to benzo[c]fluorene compounds **BF8**, **BF9** and **BF12.**

Indanone (1) was brominated by NBS[28] to 3-Bromoindanone (2), which was dehydrobrominated by triethylamine[29] to 2H-inden-1-one (3). The latter underwent self-condensation when heated in DMF,[30] forming benzo[c]fluorenone-9 (4). This compound was reduced by hydrazinehydrate in diethyleneglycol and then crystallized to benzo[c]fluorene (5).[31] The latter was methylated (methyl iodide, potassium tert-butoxide, THF) to 7,7-dimethyl-7H-benzo[c]fluorene (6).[32] A careful bromination of compound (6) led to 5,9-dibromo-7,7-dimethyl-7H-benzo[c]fluorene (7), which was passed to cross-coupling reaction with appropriate arylboronic acid giving rise to target 5,9-diaryl-7,7-dimethyl-7H-benzo[c]fluorenes (8). The arylboronic acids were obtained from aryl bromides in a usual way using their lithium derivatives and trimethylborate. The aryl bromide 9,9-dihexyl-3-bromo-9H-fluorene was obtained by alkylation of 3-bromo-9H-fluorene with 1-bromohexane, whereas the latter followed from reduced (hydrazinehydrate, potassium hydroxide, diethyleneglycol) 3-bromo-9H-fluoren-9-one.[33] Other aryl bromides (4-bromobiphenyl, 4-bromophenethole) used in the synthesis were commercially available.

The intermediate 2,7-dibromo-9-pentyl-9-(4-hexylphenyl)-9H-fluorene (14), which was utilized in the synthesis of the target compound as well as the target 2,7-bis(9,9-dihexylfluoren-3-yl)-9-pentyl-9-(4-hexylphenyl)-9H-fluorene (15) were prepared according to the Scheme 2.

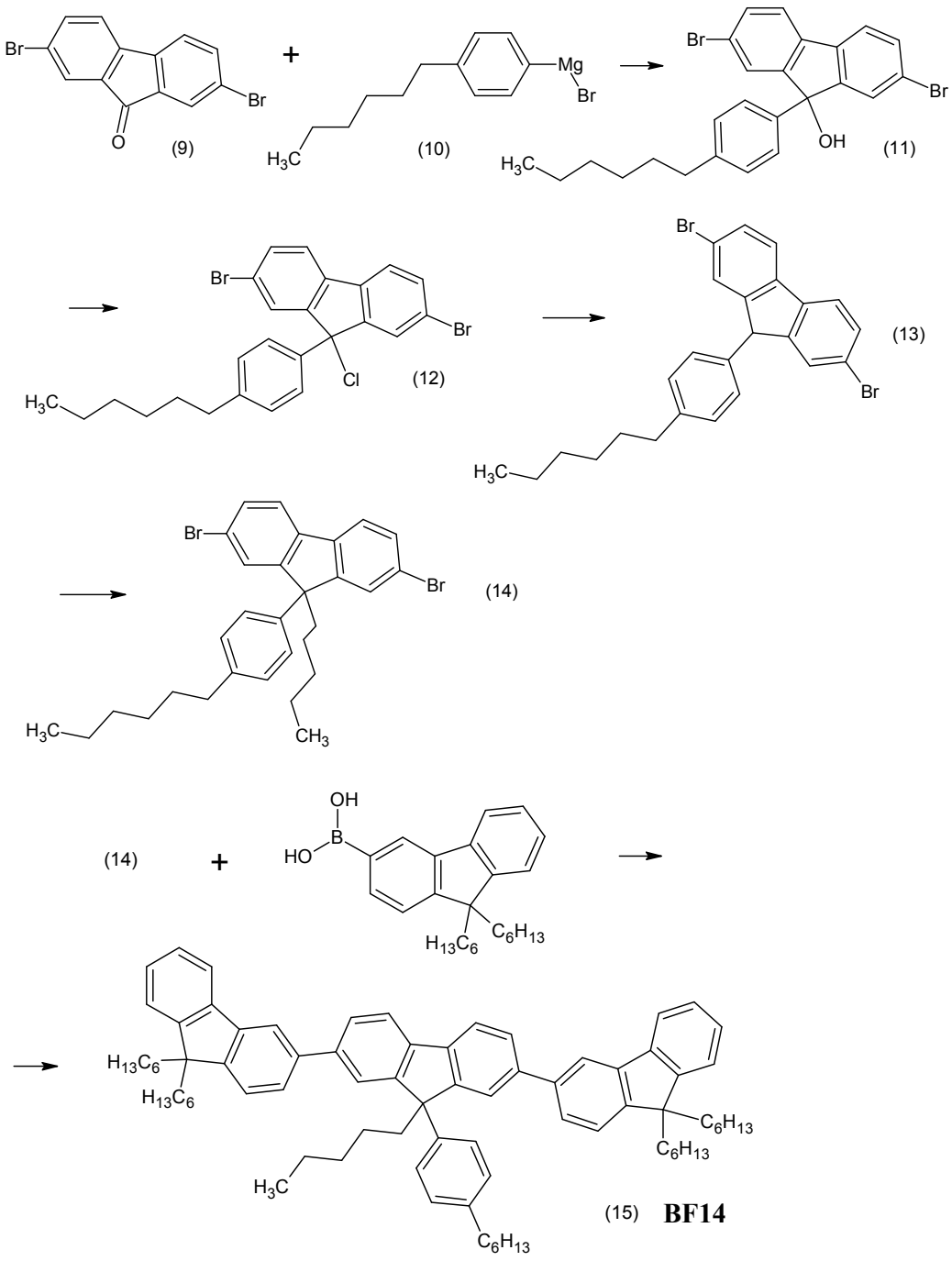

Scheme 2 Synthesis route to the reference fluorene-cored compound **BF14**.

2,7-Dibromofluorenone-9 (9) was put into reaction with 4-hexylphenylmagnesium bromide (10) obtained from 1-bromo-4-hexylbenzene. The reaction led to 2,7-dibromo-9-hydroxy-9-(4-hexylphenyl)fluorene (11), which was converted to 2,7-dibromo-9-chloro-9-(4-hexylphenyl)fluorene (12) by an action of thionyl chloride. The compound (14) was reduced by zinc powder to 2,7-dibromo-9-(4-hexylphenyl)-9H-fluorene (13), which was then alkylated by 1-

bromopentane in alkaline media to give rise to the intermediate 2,7-dibromo-9-pentyl-9-(4-hexylphenyl)-9H-fluorene (14). The intermediate (14) was passed to a reaction with 3-(9,9‘-dihexyl-9H-fluorenyl)boronic acid resulting in the target 2,7-bis(9,9-dihexylfluoren-3-yl)-9-pentyl-9-(4-hexylphenyl)-9H-fluorene (15).

3.2. Thermal properties

Thermal properties of the benzofluorenes were estimated by DSC. Fig. 1 illustrates second heating scans of DSC for all of the compounds. Estimated glass transition (T_g), crystallization (T_c) and melting (T_m) temperatures of the compounds are summarized in Table 1. Only two of the four compounds, i.e., benzfluorene **BF12** and the reference **BF14,** both featuring bulky peripheral dihexylfluorenyl moieties showed glass transition. Lower T_g (20 °C) observed for **BF14** as compared to that for **BF12** (53 °C) is mainly due to the long aliphatic chains linked to the central fluorene moiety. Higher T_g of the benzfluorene compound **BF12** implies higher thermal stability of the glassy state that is crucial for a device stability.[34] No peaks due to crystallization or melting were detected during the first and second DSC scans of the compounds **BF12** and **BF14**. Conversely, the benzofluorenes **BF8** and **BF9** with smaller phenyl-like peripheral moieties displayed crystallization/melting peaks and no traces of the glass transition (see Fig. 1 and Table 1). Two different crystallization and melting temperatures obtained for compound **BF8** are assigned to different polymorphs. The amorphous nature of the compounds **BF12** and **BF14** accompanied with relatively low T_g can be attributed to loose molecular packing mainly due to the bulky dihexylfluorenyl peripheral groups.

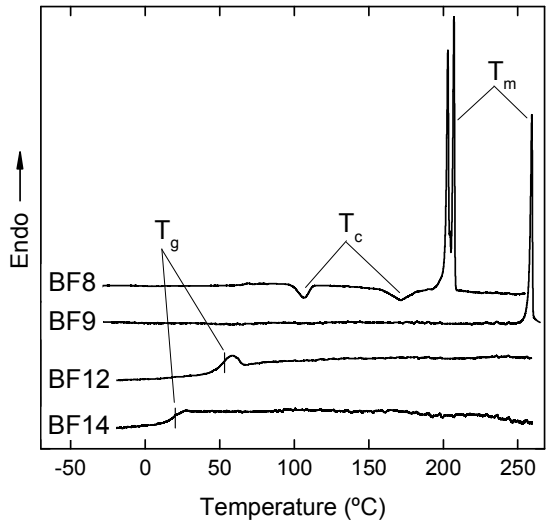

Fig. 1 DSC second-heating curves of the benzofluorenes **BF8**, **BF9**, **BF12** and the reference compound **BF14.**

Table 1 Thermal properties of the benzofluorenes **BF8**, **BF9**, **BF12** and the reference compound **BF14**.

Compound	T_g °C [a]	T_c °C [b]	T_m °C [c]
BF8	-	107, 172	203, 207
BF9	-	216	259
BF12	53	-	-
BF14	20	-	-

[a] Glass transition temperature. [b] Crystallization temperature. [c] Melting temperature.

3.3. Density functional theory calculations

Quantum chemical calculations of the benzofluorene derivatives in the gas phase were carried out using density functional theory (DFT) at the B3LYP/6-31G* level as implemented in the Gaussian 09 software package.[35] Geometry optimization revealed strongly twisted structures of the compounds in the ground state. The dihedral angles between the benzofluorene core and peripheral moieties linked to the 9th position of the core varied from 39° (for fluorenyl moiety) to 46° (for phenyl moiety), whereas the same angles for the side moieties linked to the 5th position of benzofluorene were substantially larger and varied from 53° (for dihexylfluorenyl moiety) to 69° (for phenyl moiety). The larger twisting angles were obviously induced by the naphthalene subunit of the benzofluorene core causing greater steric repulsion of the adjacent peripheral moieties. The calculated highest occupied molecular orbitals (HOMOs) and lowest unoccupied molecular orbitals (LUMOs) of the benzofluorenes **BF8**, **BF9** were found to be localized primarily on the benzofluorene core and adjacent phenyl moieties (Fig. 2). Despite the utilization of conjugated fluorenyl side moieties in the compound **BF12,** the extension of molecular orbitals remained almost unchanged, *i.e.*, the orbitals remained localized mainly on the benzofluorene core and the nearest benzene rings of the peripheral moieties. The nearly unaltered configuration of molecular orbitals could be justified by the "angular" linking topology caused by the utilization of the 3rd linking position of the fluorenyl side moieties. Similar effect was observed for 3- and 3,6-substituted carbazole derivatives.[36–38] HOMO and LUMO of the reference compound **BF14** resembled those of

BF12, however, the replacement of benzofluorene core with the fluorene obviously conditioned reduced conjugation (Fig. 2).

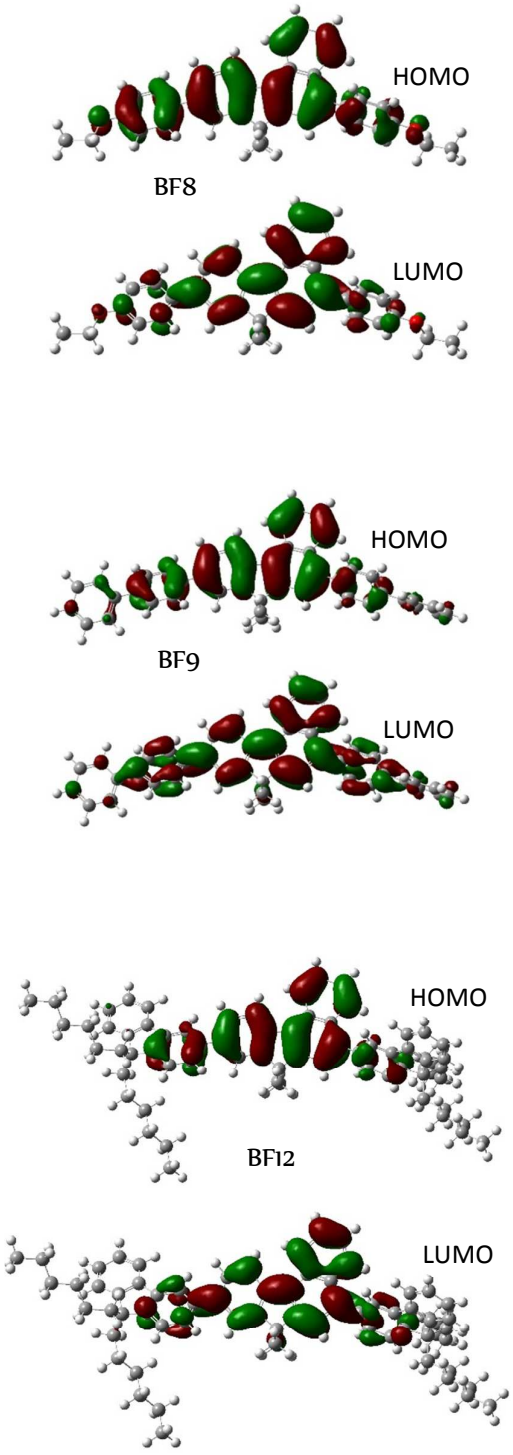

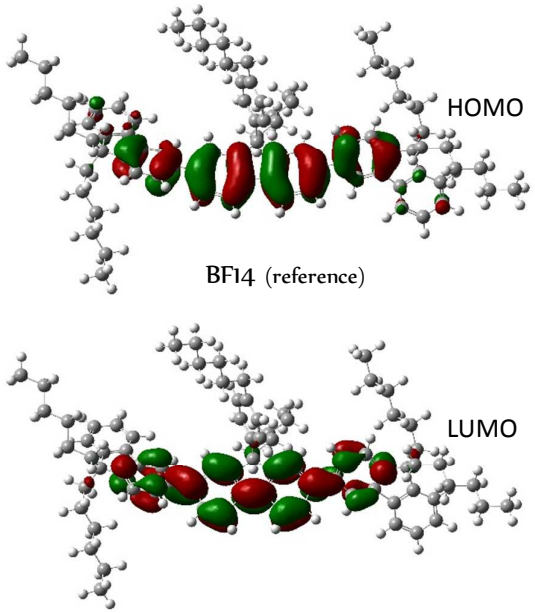

Fig. 2 HOMO and LUMO of the benzofluorene derivatives **BF8**, **BF9**, **BF12** and the reference compound **BF14** calculated using the B3LYP/6-31G* basis set.

Transition energies and oscillator strengths of the compounds were calculated using time-dependent DFT (TD-DFT) approach. The parameters involving two lowest singlet and triplet states are summarized in Table 2. The calculations indicate the dominant $S_0 \rightarrow S_1$ transitions for all the compounds with oscillator strengths of about two orders of magnitude larger as those of $S_0 \rightarrow S_2$. The energies of the dominant transitions are located in the UV (3.46 – 3.67 eV). They are found within 20 meV for compounds **BF8** and **BF9**, whereas the transition energy of compound **BF12** bearing conjugated fluorenyl side moieties is by more than 100 meV lower as compared to those of **BF8** and **BF9**. On the other hand, the lowest transition energy of the reference **BF14** bearing fluorene core is ~300 meV higher in respect to that of analogous benzofluorene compound **BF12** due to the reduced conjugation of the core. The oscillator strengths of the lowest singlet transitions of compounds **BF12** and **BF14** are evidently larger as compared to those of **BF8** and **BF9** pointing out the importance of peripheral fluorenyl moieties. S_2 state for the benzofluorene compounds is found to be by 0.35 – 0.65 eV higher in energy, meanwhile T_1 by ~1.0 eV lower in energy in respect to S_1 state. The latter value indicates large singlet-triplet splitting in these molecules originating from excellent HOMO and LUMO overlap.[39]

Table 2 Calculated transition energies and oscillator strengths for the two lowest spin-allowed and spin-forbidden transitions of the benzofluorene compounds.

Compd.	$S_0 \rightarrow S_1$		$S_0 \rightarrow S_2$		$S_0 \rightarrow T_1$	$S_0 \rightarrow T_2$
	E (eV) [a]	f [b]	E (eV) [a]	f [b]	E (eV) [a]	E (eV) [a]
BF8	3.459	0.67	4.002	0.0033	2.365	3.272
BF9	3.443	0.81	4.088	0.0032	2.315	3.260
BF12	3.367	1.12	3.819	0.0173	2.281	2.927
BF14	3.674	1.66	4.021	0.0046	2.653	2.990

[a] Transition energy. [b] Oscillator strength.

3.4. Absorption and emission spectra

Absorption and fluorescence spectra of the dilute THF solutions and neat films of benzofluorene compounds are displayed in Fig. 3. The details of the optical properties are listed in Table 3. The studied benzofluorenes absorb in the UV spectral range (absorption maxima varies from 358 nm to 380 nm) while emit in the deep blue range (403 – 418 nm). Note a good agreement between experimentally determined $S_0 \rightarrow S_1$ absorption energies and the transition energies obtained from TD-DFT calculations. Obviously, the spectra of compounds are shifted to longer wavelengths as compared to those of single fluorene moiety[40] as a result of the enhanced conjugation of benzofluorene core. Indeed, the spectra of the reference compound **BF14** containing fluorene core have peaks similar to those of single fluorene moiety. This is caused by the large twisting of sterically hindered peripheral groups and by utilization of the 3rd linking position of the fluorenyl side moieties, which disrupt the conjugation in **BF14**. The compounds **BF8** and **BF9** exhibit very similar shapes and spectral positions of absorption and fluorescence bands in solutions, whereas the compound **BF12** shows almost 2-fold increase in absorbance and the redshift of absorption band (by 20 nm) as compared to **BF8** and **BF9.** This increase in absorbance nicely correlates with a similar enhancement in oscillator strength revealed by TD-DFT calculations. These differences in **BF12** arise due to the presence of more conjugated fluorenyl peripheral groups. Interestingly, the fluorescence band of benzofluorene **BF12** has similar spectral location as that of **BF8** and **BF9** indicating minor role of dihexylfluorenyl peripheral groups in the excited state.

Fluorescence spectra of the neat films of benzofluorene derivatives are shifted to the long wavelengths as compared to those of dilute solutions due to the intermolecular interactions. The larger bathochromic shifts (~20 nm) and, consequently, stronger intermolecular coupling were observed for the compounds **BF8** and **BF9** featuring smaller phenyl-like peripheral groups as

compared to those of **BF12** and **BF14.** The latter compounds exhibited negligible bathochromic shifts amounting to only 3 nm as a result of the bulky dihexylfluorenyl peripheral groups acting as spacers, and thus, weakening intermolecular interaction.

Fluorescence quantum yield (Φ_F) of the non-interacting benzofluorene molecules in dilute solutions was found to be rather high and ranged from 63% to 72%. Φ_F for the fluorene-cored reference **BF14** was slightly smaller, 60% (see Table 3). Interestingly, high Φ_F (38 – 45%) was also observed for the neat films of benzofluorenes irrespectively of their peripheral moieties. Less than 2-fold decrease of Φ_F in the neat films suggested weak concentration quenching, which was further explored in the next section.

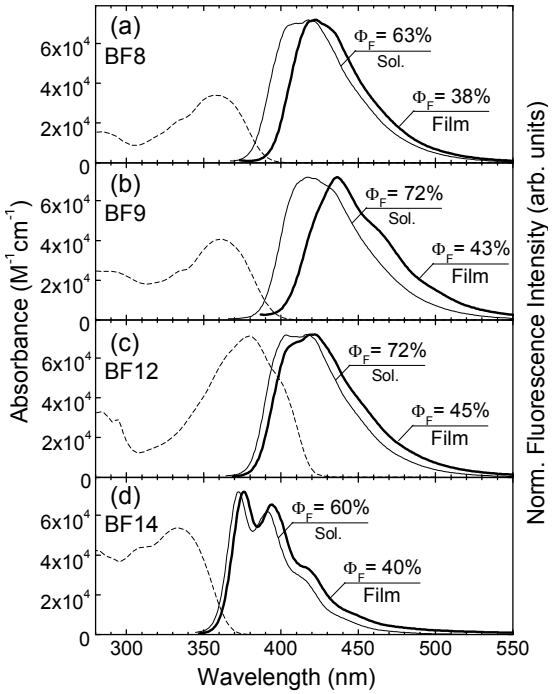

Fig. 3 Absorption (dashed line) and fluorescence spectra of the benzofluorenes (a) **BF8**, (b) **BF9**, (c) **BF12**, and the reference compound (d) **BF14** in 10^{-5} M THF solutions (thin solid line) and neat films (thick solid line). Fluorescence quantum yields, indicated.

For light-emitting devices triplet energies of the compounds serving as guests or hosts are of crucial importance,[39,41] however they can be also important for lasing materials. Owing to the long lifetimes of the lowest-energy triplets, they are likely to be populated in electrically-driven lasers operating in continuous-wave, and thus may participate in the triplet absorption.[7,11] Triplet state

energies (E_T) of the benzofluorenes were evaluated from the position of 0th vibronic band of the phosphorescence spectra measured at 20 K (see Fig. S1 in the Supplementary Information and the explanation therein). E_T values of the compounds are listed in Table 3.

Table 3 Optical properties of the benzofluorene compounds in dilute (10^{-5} M) THF solutions and neat films. Phosphorescence data were obtained for the compounds dispersed in PS matrix at the concentration of 1 wt %.

	Dilute THF solution							Neat film			Phosphoresc.
	λ_{abs} (E_{S1}) [a]	ε [b]	λ_F [c]	Φ_F [d]	τ [e]	k_r [f]	k_{nr} [g]	λ_F [c]	Φ_F [d]	τ [e]	λ_{Ph} (E_{T1}) [h]
Compd.	nm (eV)	l mol^{-1} cm^{-1}	nm	%	ns	$\times 10^8$ s^{-1}	$\times 10^8$ s^{-1}	nm	%	ns	nm (eV)
BF8	358 (3.462)	34000	403	63	1.5	4.2	2.5	422	38	0.8 [64%]	587 (2.112)
			418							2.6 [36%]	
BF9	360 (3.443)	40600	418	72	1.1	6.5	2.5	436	43	0.5 [88%]	589 (2.104)
										1.5 [12%]	
BF12	380 (3.279)	71000	403	72	1.3	5.5	2.2	406	45	0.5 [93%]	580 (2.137)
			416					420		2.3 [7%]	
BF14	335 (3.700)	53600	373	60	0.9	6.7	4.4	376	40	0.4 [68%]	515 (2.407)
										0.8 [29%]	
										5.3 [3%]	

[a] Absorption band maximum. [b] Molar extinction coefficient. [c] Fluorescence band maximum. [d] Fluorescence quantum yield. [e] Excited state lifetime. [f] Radiative relaxation rate. [g] Nonradiative relaxation rate. [h] Phosphorescence band maximum at 20 K.

3.5. Excited state dynamics

Excited state relaxation dynamics of the benzofluorenes was assessed by measuring fluorescence transients of their dilute solutions and neat films (Fig. 4). The dilute solutions of **BF8**, **BF9** and **BF12** exhibited single exponential decay with a similar decay time constants (τ) of 1.1 − 1.5 ns, which are typical of organic fluorophores. The reference **BF14** bearing fluorene core showed slightly shorter τ of 0.9 ns. Fluorescence transients of the neat films expressed clearly nonexponential behavior with faster excited state relaxation occurring during the first 3-4 ns after excitation pulse and a slower relaxation at a later stage (ca. 4 ns after excitation). The nonexponential temporal profile accompanied by the redshifted fluorescence bands in the solid films indicated energy transfer arising via exciton hopping through the localized states in disordered or partly disordered media.[42] The fluorescence decay profiles were fitted by using two- or three-

component exponential decay models to reveal the major component and its fractional intensity (see Table 3). The fractional intensity of the component signifies its actual contribution to the overall excited-state decay and is indicated in the brackets next to the τ value. Evidently, the major contribution was afforded by the fast component with $\tau < 1.0$ ns. τ of the component was roughly half as that obtained in solution and could be associated mainly with nonradiative relaxation induced by exciton migration in the solid phase at the early decay stage.[43,44] This was also supported by the reduced Φ_F in the neat films amounting to < 50% and signifying the nonradiative decay channel as the governing one. Meanwhile, the slower decay component could be attributed to stronger localized excitons capable of evading fast nonradiative decay. Generally, more pronounced exciton migration, and thus migration-induced fluorescence quenching accompanied by the excited state lifetime shortening is expected for more ordered films with the tighter molecular packing.[27,45] Therefore, bulky peripheral groups such as dihexylfluorenyl moieties in the benzofluorene **BF12** and the reference **BF14** should cause much less ordered, *i.e*, amorphous films as compared to more dense films of **BF8** and **BF9.** However, no significant differences among the benzofluorene compounds in Φ_F quenching or shortening of the major component of τ in the neat films were observed (see Table 3).

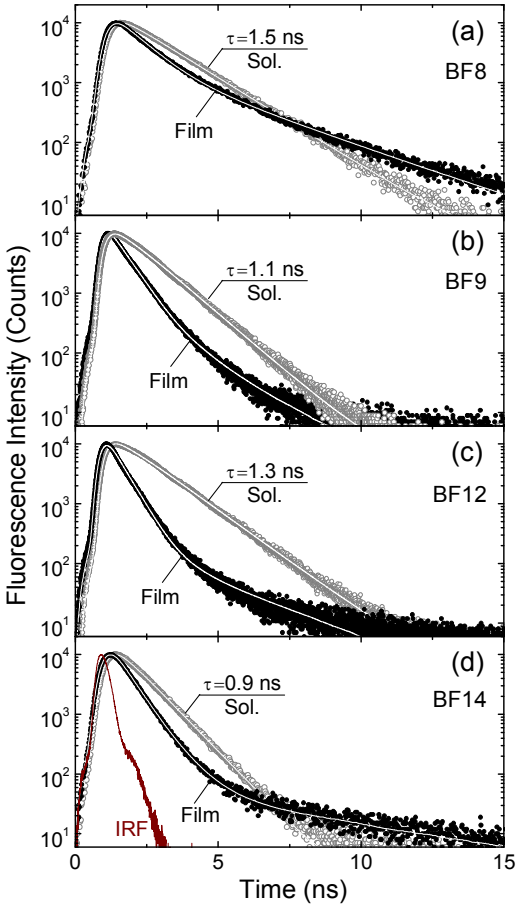

Fig. 4 Fluorescence transients of the benzofluorenes (a) **BF8**, (b) **BF9**, (c) **BF12**, and the reference compound (d) **BF14** in 10^{-5} M THF solutions (grey circles) and neat films (black points). Lines mark exponential or multiexponential fits to the experimental data. Instrument response function (IRF) and fluorescence lifetimes for solutions, indicated.

Calculations of radiative and nonradiative relaxation rates, k_r and k_{nr} respectively, by using the relations $k_r = \Phi_F/\tau$, $k_{nr} = (1-\Phi_F)/\tau$ yielded similar k_{nr} of ~2.5×10^8 s^{-1} and only slightly different k_r [$(4.2 - 6.5)\times10^8$ s^{-1}] for benzofluorenes **BF8**, **BF9** and **BF12** in dilute solutions. For comparison, the fluorene-cored reference **BF14** exhibited somewhat larger k_r, but also nearly twice as large k_{nr}. Large k_r is important for lasing materials as it allows attaining low ASE threshold.[46]

3.6. Concentration quenching

High radiative relaxation rates and emission efficiencies are essential for achieving low ASE threshold in lasing materials.[47] Preserving these properties at high chromophore concentration is just as important for realization of efficient laser.[1] The concentration quenching of the benzofluorene derivatives was investigated by evaluating Φ_F of the compounds dispersed in polystyrene matrix as a function of their concentration from 0.5 to 100 wt % (Fig. 5). At low concentrations in PS matrix all the benzofluorene compounds exhibited similar Φ_F (70 – 80%), which were up to 10% higher as compared to those estimated in dilute solutions. The slight enlargement of Φ_F could be attributed to the suppressed intramolecular torsions in the environment of increased rigidity.[48,49] It is worth highlighting that increasing compound concentration up to 10 wt % in PS matrix had negligible influence on the fluorescence efficiency, whereas further increase of the concentration up to 100 wt % resulted in about 2-fold drop of Φ_F. Similar tendency was also obtained for average fluorescence lifetime (τ_{avg}) estimated independently from Φ_F (see Fig. 5). Roughly, similar behavior and drop of τ_{avg} with increasing compound concentration were observed for all the benzofluorenes. The simultaneous reduction of both Φ_F and τ_{avg} could only be justified by the enhanced nonradiative processes originating from increased intermolecular coupling at high compound concentration. Enhanced intermolecular coupling facilitates exciton migration to the quenching (or so-called "dark") states consequently promoting the nonradiative deactivation. The "dark" states are commonly associated with non-emissive molecular aggregates, however, even in the absence of aggregation, *e.g.* in purely amorphous films, excimer species, intrinsic defects, distortions or other non-intentionally added quenching defects such as impurity traps might also serve as the "dark" states. Essentially, the concentration quenching effect of the benzofluorenes **BF8**, **BF9, BF12**, and the reference compound **BF14** is weak, and moreover, the degree of quenching does not depend notably on peripheral groups. For comparison, well-known bay-substituted perylene diimide dyes exhibited huge concentration quenching resulting in more than 10-fold reduction of Φ_F already at the concentration of 10 wt %.[50] The 10-fold drop of Φ_F with increasing compound percentage in PS up to 100 wt % was obtained for triphenylamine derivatives[27] and also for diphenylanthracene-based compounds.[51] The weak quenching of the studied benzofluorene compounds can be attributed to their twisted molecular geometries resulting from singly-bridged multi-fragment structures and to a lesser extent to the volume of peripheral moieties.

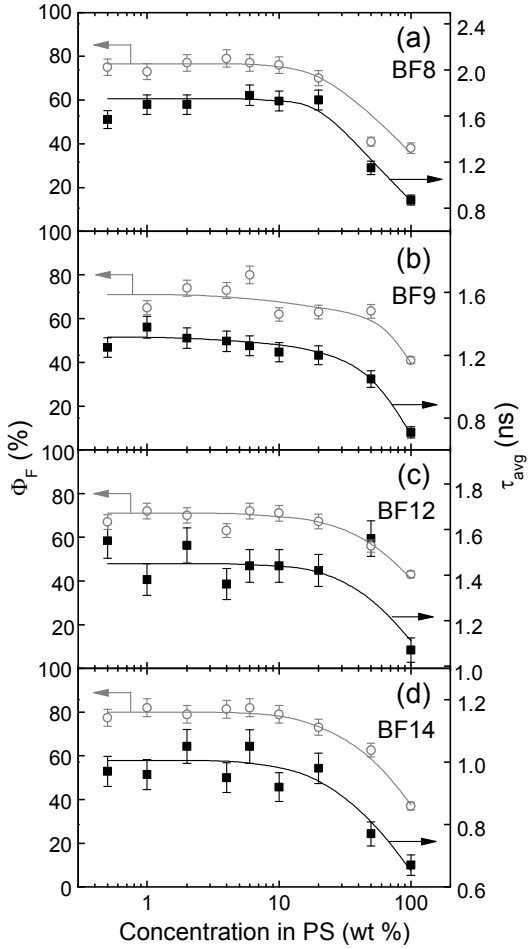

Fig. 5 Fluorescence quantum yields (grey circles) and average fluorescence lifetimes (black rectangles) of the benzofluorenes (a) **BF8**, (b) **BF9**, (c) **BF12**, and the reference compound (d) **BF14** as a function of their concentration in PS matrix.

3.7. Amplified spontaneous emission

The potential of benzofluorenes for light amplification was tested by carrying out amplified spontaneous emission (ASE) measurements in one of the simplest mirrorless configurations, the so-called thin excitation stripe configuration. This is by far the most appropriate technique used to compare the performance of different materials for lasing application excluding resonant cavity effects, *i.e.* external resonators or distributed feedback gratings.[9] The technique is based on the excitation of slab waveguide samples with a pulsed laser stripe and registration of emission spectra

from a sample edge.[22,23] Essentially, spontaneous emission travelling along the excitation path (stripe) is amplified by the stimulated transitions causing spectral narrowing of the emission above certain pump intensity referred to as ASE threshold (I_{th}^{ASE}).

ASE of the benzofluorenes was investigated as a function of their concentration in PS matrix to reveal the impact of intermolecular coupling, possible aggregate formation on the ASE performance. Importantly, all the compounds expressed ASE in their neat films, which is often difficult to achieve due to the strong concentration quenching of emission.[52,53] Fig. 6 shows excitation power dynamics of the edge emission spectra of the neat films of benzofluorenes **BF8**, **BF9**, **BF12**, and the reference compound **BF14**. At the lowest pump density all the compounds demonstrate broad spontaneous emission band, which spectrally narrows with the onset of ASE. The ASE peaks appear redshifted by 5 – 20 nm in respect to the spontaneous band maxima due to the absorptive losses at the short-wavelength slope of emission spectra (reabsorption effect). The sudden emission band narrowing with the increasing pump is accompanied by an abrupt change in the emission intensity from linear to superlinear at I_{th}^{ASE} (see insets of Fig. 6). The notable deviation from the linear to sublinear dependence of emission intensity *vs* pump was observed for **BF9** below I_{th}^{ASE}. This was caused by the enormously high I_{th}^{ASE} (200 kW/cm^2) obtained for the neat film of **BF9,** which implied utilization of high pump fluences in ASE measurements eventually resulting in gradual material and emission degradation.

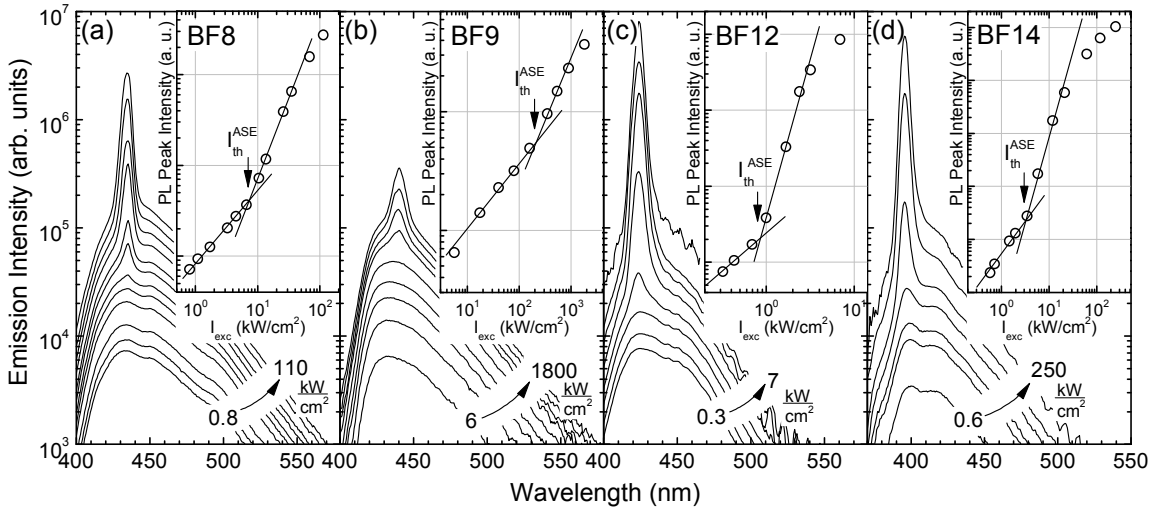

Fig. 6 Excitation power dependence of the edge emission spectra of the neat films of benzofluorenes (a) **BF8**, (b) **BF9**, (c) **BF12**, and the reference compound (d) **BF14**. Insets show emission peak intensity *vs* excitation power density (I_{exc}). Lines are guides for the eye. Arrows indicate onset of ASE.

Concentration dependence of I_{th}^{ASE} for the studied benzofluorenes and the reference compound dispersed in PS matrix are illustrated in Fig. 7a. Elucidation of this dependence is crucial for determination of the optimal compound concentration for laser operation.[54–57] Moreover, I_{th}^{ASE} is one of the key parameters describing the feasibility of the material to be employed in lasing systems as an active medium. Generally, the benzofluorenes **BF8, BF9** and **BF12** show different behavior of I_{th}^{ASE} with increasing concentration. I_{th}^{ASE} decreases for all the compounds up to the concentration of 5 wt %. Further on, it continues to decrease for **BF12** as well as for the reference **BF14** up to the highest concentrations, whereas for the compounds **BF8** and **BF9,** the saturation and even steep increase of I_{th}^{ASE}, respectively, is observed just above 5 wt %. The decrease of I_{th}^{ASE} with increasing concentration is related to the reduction of optical losses due to the reduced intermolecular distances. Higher compound concentration in PS matrix facilitates attaining of critical exciton density required to achieve I_{th}^{ASE}. Note that at low concentrations (<5 wt %) the studied benzofluorenes exhibit similar I_{th}^{ASE}. This can be explained by the inverse proportionality of I_{th}^{ASE} to Einstein's coefficient B, which directly relates to k_r as $B \propto (c^3/8\pi h \nu_0^3)k_r$, where h is Planck's constant, ν_0 is the frequency of light, and c is the velocity of light.[46] The insignificant differences in k_r obtained for the benzofluorenes **BF8**, **BF9** and **BF12** in dilute solutions (see Table 3) therefore correspond to small variations in I_{th}^{ASE}. Taking into account that k_r values were estimated for the dilute solutions, the similarity of I_{th}^{ASE} pertains only to low compound concentrations.

For compounds **BF12** and **BF14** the lowest I_{th}^{ASE} was attained at their highest concentrations in PS matrix, *i.e.*, in their neat films (see Fig. 7a). In contrast, for **BF9** the lowest I_{th}^{ASE} was achieved at the concentration of ~6 wt %. However, the steep increase of I_{th}^{ASE} with further increasing concentration could not be related to concentration quenching, because it was found to be weak and similar for all the benzofluorenes studied (see Fig. 5). Examination of the PS films with high **BF9** concentration under optical microscope in the dark field enabled to discern (sub)micron size aggregates, which are displayed in Fig. 7b for the neat film. The aggregates had a tendency to increase in size with increasing concentration, and obviously, were a prime cause of drastically enlarged I_{th}^{ASE} due to the increased scattering of directional ASE. Aggregation-induced absorption in the spectral region of the amplified emission might also contribute to the enlarged I_{th}^{ASE}. However in this case it can be ruled out, since all the benzofluorenes demonstrate similar concentration quenching (see Fig. 5) and similar Φ_F of the neat films signifying negligible role of aggregates in emission quenching.

Similar aggregate formation, although of greatly reduced extent was identified in the PS films of **BF8** at high concentrations. Most likely, the saturation of I_{th}^{ASE} above ~6 wt % for **BF8** was caused by the competing processes of reduced intermolecular separation (conditioning reduced optical losses) and aggregation-induced scattering of amplified emission (conditioning increased losses). No traces of aggregation were detected in the neat films of **BF12** and **BF14** verifying their amorphous nature as revealed from DSC measurements (see Fig. 1). The amorphous morphology of the neat films of compounds **BF12** and **BF14** was also confirmed by atomic force microscopy (see Fig. S2 in the Supplementary Information). Evidently, the bulky dihexylfluorenyl peripheral moieties in the compounds **BF12** and **BF14**, conversely to the smaller phenyl-like moieties, are able to suppress aggregation, and hence, aggregation-induced light scattering.

The lowest ASE threshold obtained in the neat film of benzofluorene **BF12** (I_{th}^{ASE} = 900 W/cm^2) indicates advantage over analogous fluorene-cored compound **BF14** demonstrating somewhat higher I_{th}^{ASE} (3 kW/cm^2) in the neat film. This can be attributed partly to the larger extinction coefficient of **BF12** assuming similar packing density of the neat films (see Table 3). I_{th}^{ASE} value of 900 W/cm^2 (4.5 μJ/cm^2) achieved for the benzofluorene film in air was found to be comparable or lower than, *e.g.* that reported for polyspirobifluorenes (4.4 μJ/cm^2),[58] oligofluorenes (9 - 16 μJ/cm^2),[59,60] various bisfluorene-cored dendrimers (16 – 50 μJ/cm^2),[61] poly(9,9-dioctylfluorene) (29 μJ/cm^2)[62] etc., measured under similar nanosecond excitation in a mirrorless configuration. Still, this I_{th}^{ASE} value was an order of magnitude higher as compared to possibly the lowest ever reported I_{th}^{ASE} value (0.43 μJ/cm^2) attained in the neat film of 2,7-bis[4-(N-carbazole)phenylvinyl]-9,9′-spirobifluorene.[16] Note however that the record energy threshold value was obtained by using the shorter pulse (500 ps) excitation source, which implied nearly the same threshold density value for power (860 W/cm^2) as that achieved by us in benzofluorene **BF12**. Moreover, unlike in our case, where ASE measurements were performed in air, the record value was obtained in a nitrogen atmosphere with the photooxidative degradation eliminated. Taking this into account, such low ASE threshold achieved in the neat film prepared from solution by spin-coating in air shows great potential for benzofluorene-cored molecular glasses as active media for lasing applications.

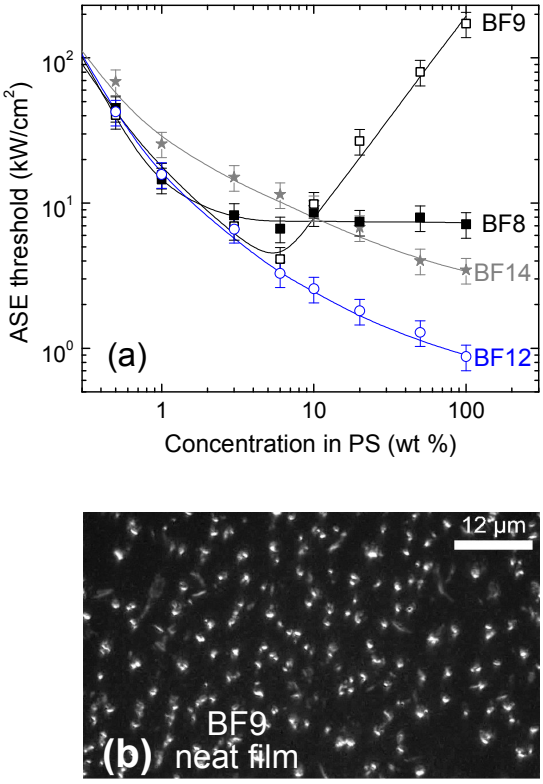

Fig. 7 (a) ASE threshold as a function of compound **BF8**, **BF9**, **BF12** and **BF14** concentration in a PS matrix. Lines are guides for the eye. (b) Dark field optical image of the neat film of **BF9**.

Table 4 Amplified spontaneous emission properties of the benzofluorene compounds.

	λ_{ASE} [a]	I_{th}^{ASE} [b]	$t_{1/2}^{ASE}$ [c]
Compound	nm	kW/cm^2	pump pulses
BF8	435	8 (neat film)	8×10^3 @16 kW/cm^2
BF9	440	4 (6 wt % in PS)	9×10^3 @8 kW/cm^2
BF12	424	0.9 (neat film)	20×10^3 @1.8 kW/cm^2
BF14	395	3 (neat film)	5×10^3 @6 kW/cm^2

[a] ASE band maximum. [b] ASE threshold. [c] Photostability lifetime.

3.8. Photostability

Photostability is important for lasing materials for it allows maintaining sufficiently high photon flux in operating conditions. The photostability of the benzofluorene compounds was assessed by monitoring ASE intensity as a function of the number of pump pulses at the constant pump density in an ambient atmosphere (Fig. 8). The compound concentrations in PS matrix resulting in the lowest I_{th}^{ASE} were chosen for these measurements. To approach the real working conditions of a laser device, the measurements were performed at the pump density equal to $2 \times I_{th}^{ASE}$. All the studied compounds exhibited drop in the total ASE output with the number of pump pulses indicating material degradation. The degradation is commonly associated with the photooxidation, *i.e.*, creation of carbonyl defects (also known as keto defects in fluorene-based compounds)[63] in the active medium leading to a quenching of emission as well as the optical loss at the pump wavelengths.[7,10] The photostability of the benzofluorenes was compared by comparing their stability lifetimes ($t_{1/2}^{ASE}$) defined as the number of pump pulses resulting in a drop of ASE intensity to half its initial value (see Table 4). The estimated $t_{1/2}^{ASE}$ for the benzofluorenes **BF8**, **BF9** and **BF12** varied from 8×10^3 to 20×10^3 pulses and was comparable to the lifetimes of other small-molecules or polymers evaluated under similar conditions (in nanosecond/picosecond pulse regime).[50,64]

The largest $t_{1/2}^{ASE}$ of 20×10^3 pump pulses, and thus the highest photostability was determined for the neat film of benzofluorene **BF12.** This is mainly because of the significantly reduced ASE threshold as compared to that of the rest compounds (see Table 4). The fluorene-cored reference compound **BF12** exhibited the worst photostability with $t_{1/2}^{ASE}$ of 5×10^3 pulses suggesting the fluorene to be more prone to photooxidation in respect to benzofluorene. The latter result shows the advantage of benzofluorene derivatives against fluorene compounds in terms of photostability for lasing applications.

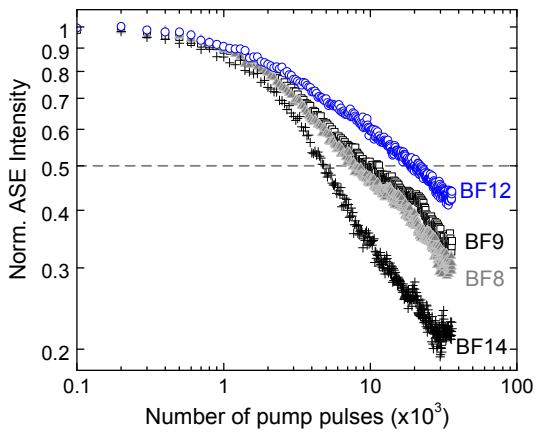

Fig. 8 Normalized ASE intensity dependence on the number of pump pulses for benzofluorenes **BF8**, **BF9**, **BF12**, and the reference **BF14** dispersed in PS matrix at the concentration corresponding to the lowest I_{th}^{ASE}, *i.e.*, 100, 6, 100 and 100 wt%, respectively. The excitation power densities were $2 \times I_{th}^{ASE}$, *i.e.*, 16, 8, 1.8 and 6 kW/cm^2, respectively.

3.9. Carrier drift mobility

Lasing materials of high carrier mobility are required to ensure sufficiently high current densities through a device, and subsequently, to attain sufficient exciton concentrations for achieving stimulated emission.[1] Carrier drift mobilities of the wet-casted neat films of the benzofluorenes were measured by xerographic time-of-light (XTOF) technique in vacuum at room temperature. Unfortunately, the XTOF measurements for compound **BF9** were impossible as the film readily crystallized upon casting. The neat film of the reference **BF14** featuring low T_g (20 °C) was by far too soft resulting in film thickness changes under applied electric field making the measurements unreliable. Fig. 9a shows representative *dU*/*dt* hole-transients at different applied voltages for the neat film of compound **BF8**. The transit time (t_t) of the carriers determined from the kink in the double logarithmic plot of *dU*/*dt* was used to deduce the drift mobility (μ_h) according to the formula $\mu_h = d^2/U_0 t_t$, where d is the sample thickness and U_0 is the surface potential at the moment of the excitation. The compound exhibited a dispersive hole transport, which was accompanied by the substantial increase of μ_h with the electric field (see Fig. 9b) indicating importance of energetic disorder in the trap-dominant transport.[65] The benzofluorene **BF8** exhibited rather high μ_h of 2×10^{-3} cm^2/Vs at an electric field of 0.5 MV/cm, whereas **BF12** expressed only moderate μ_h (8×10^{-5} cm^2/Vs) at the same conditions. Significantly lower μ_h estimated for the neat film of **BF12** is attributed to a loose molecular packing caused by the bulky dihexylfluorenyl peripheral groups. Thus, although the bulky groups at periphery ensure formation of aggregate-free amorphous films with ASE scattering due to aggregates avoided, and hence ASE threshold reduced, they obviously deteriorate carrier drift mobility hampering material utilization in organic lasers. On the other hand, the more compact ethoxyphenyl peripheral moieties in **BF8** facilitate denser packing thereby enhancing carrier transport. However, the dense packing facilitates formation of aggregates in the films (see Fig. S2 in the Supplementary Information), which act as ASE scatterers causing increased

ASE threshold. This implies a certain tradeoff between ASE threshold and charge transport properties for lasing materials employed as neat films.

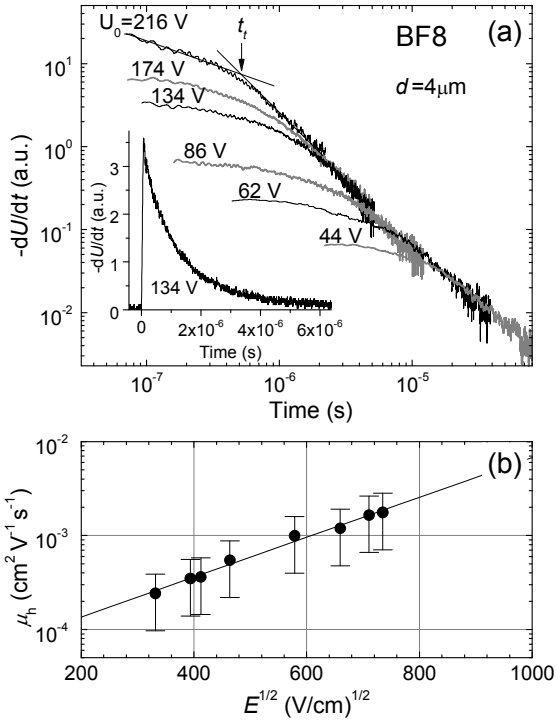

Fig. 9 (a) XTOF transients in a double logarithmic scale for the neat film of **BF8**. Arrow indicates hole transit time at U_0 = 216 V. Inset shows a typical transient curve in a linear scale. (b) Hole drift mobility (μ_h) *vs* the square root of electric field for the neat film of **BF8**. Line is exponential approximation of the experimental data.

4. Conclusion

A series of low-molecular-weight compounds utilizing benzo[c]fluorene core and emitting in the deep-blue spectral range were synthesized and studied as potential lasing materials. The compounds bearing dihexylfluorenyl and phenyl-like peripheral moieties expressed weak concentration quenching of emission as a result of the significant steric hindrance confirmed by DFT calculations. High emission quantum yield (~80%) was preserved up to the concentrations of 10 wt % in polymer matrix and was reduced only by a factor of 2 in the neat films. ASE properties assessed in the so-

called mirrorless configuration enabled to reveal intrinsic potential of benzofluorene compounds as low ASE threshold (I_{th}^{ASE}) media for lasing applications. The weak concentration quenching accompanied by high radiative decay rates (>4×10^8 s^{-1}) ensured the lowest I_{th}^{ASE} (900 W/cm^2) to be achieved in the neat amorphous films, which were spin-coated from solution in an ambient atmosphere. Interestingly, the appearance of aggregates had minimal impact on the emission efficiency of benzofluorene films, meanwhile the aggregates severely enhanced scattering of directional ASE thus dramatically increasing I_{th}^{ASE}. Utilization of bulky dihexylfluorenyl groups at the periphery prevented aggregation and favored formation of homogeneous glassy benzofluorene films with markedly reduced I_{th}^{ASE}. However, conversely to the smaller ethoxyphenyl peripheral moieties, dihexylfluorenyl groups caused more loose molecular packing lowering carrier drift mobility by a factor of 20, and thus, implying a tradeoff between ASE and charge transport properties of the lasing materials utilized in the neat form. Additionally, the neat films of benzofluorenes demonstrated photostability lifetimes ($t_{1/2}^{ASE}$) of up to 2×10^4 pump pulses under ambient conditions and were found to be more stable as compared to the films of similar fluorene-cored compounds.

Acknowledgement

The research was funded by a grant No. VP1-3.1-ŠMM-10-V-02-023 from the European Social Fund Agency. E.R. acknowledges support by project "Promotion of Student Scientific Activities" (VP1-3.1-ŠMM-01-V-02-003) from the Research Council of Lithuania. A. Vaitkevičius is acknowledged for AFM measurements.

References

1 J. Clark and G. Lanzani, *Nat Photon*, 2010, **4**, 438–446.

2 S. Chénais and S. Forget, *Polym. Int.*, 2012, **61**, 390–406.

3 S. R. Forrest, *Nature*, 2004, **428**, 911–918.

4 L. Duan, L. Hou, T.-W. Lee, J. Qiao, D. Zhang, G. Dong, L. Wang and Y. Qiu, *J. Mater. Chem.*, 2010, **20**, 6392–6407.

5 I. D. W. Samuel and G. A. Turnbull, *Chem. Rev.*, 2007, **107**, 1272–1295.

6 V. G. Kozlov and S. R. Forrest, *Curr. Opin. Solid St. M.*, 1999, **4**, 203–208.

7 C. Grivas and M. Pollnau, *Laser Photonics Rev.*, 2012, **6**, 419–462.

8 C. Karnutsch, C. Pflumm, G. Heliotis, J. C. deMello, D. D. C. Bradley, J. Wang, T. Weimann, V. Haug, C. Gärtner and U. Lemmer, *Appl. Phys. Lett.*, 2007, **90**, 131104.

9 N. Tessler, *Adv. Mater.*, 1999, **11**, 363–370.

10 G. Kranzelbinder and G. Leising, *Rep. Prog. Phys.*, 2000, **63**, 729.

11 M. D. McGehee and A. J. Heeger, *Adv. Mater.*, 2000, **12**, 1655–1668.

12 Y. C. Kim, T. -W Lee, O. O. Park, C. Y. Kim and H. N. Cho, *Adv. Mater.*, 2001, **13**, 646–649.

13 M. A. Baldo, R. J. Holmes and S. R. Forrest, *Phys. Rev. B*, 2002, **66**, 035321.

14 M. Pope and C. E. Swenberg, *Electronic Processes in Organic Crystals and Polymers*, Oxford University Press, New York, 2 edition., 1999.

15 R. Xia, G. Heliotis, Y. Hou and D. D. C. Bradley, *Org. Electron.*, 2003, **4**, 165–177.

16 H. Nakanotani, S. Akiyama, D. Ohnishi, M. Moriwake, M. Yahiro, T. Yoshihara, S. Tobita and C. Adachi, *Adv. Funct. Mater.*, 2007, **17**, 2328–2335.

17 S. Krotkus, K. Kazlauskas, A. Miasojedovas, A. Gruodis, A. Tomkeviciene, J. V. Grazulevicius and S. Jursenas, *J. Phys. Chem. C*, 2012, **116**, 7561–7572.

18 K.-S. Kim, Y.-M. Jeon, J.-W. Kim, C.-W. Lee and M.-S. Gong, *Organic Electronics*, 2008, **9**, 797–804.

19 S. O. Jeon, K. S. Yook, C. W. Joo and J. Y. Lee, *Org. Electron.*, 2010, **11**, 881–886.

20 H. Liang, X. Wang, X. Zhang, Z. Ge, X. Ouyang and S. Wang, *Dyes Pigm.*, 2014, **108**, 57–63.

21 J. C. de Mello, H. F. Wittmann and R. H. Friend, *Adv. Mater.*, 1997, **9**, 230–232.

22 K. L. Shaklee and R. F. Leheny, *Appl. Phys. Lett.*, 1971, **18**, 475–477.

23 K. Kazlauskas, G. Tamulaitis, A. Žukauskas, T. Suski, P. Perlin, M. Leszczynski, P. Prystawko and I. Grzegory, *Phys. Rev. B*, 2004, **69**, 245316–245324.

24 P. M. Borsenberger, *Organic Photoreceptors for Xerography*, Marcel Dekker, New York, 1998.

25 E. Montrimas, V. Gaidelis and A. Pazera, *Lith. J. Phys.*, 1966, **6**, 569–578.

26 R. R. Reghu, J. V. Grazulevicius, J. Simokaitiene, A. Miasojedovas, K. Kazlauskas, S. Jursenas, P. Data, K. Karon, M. Lapkowski, V. Gaidelis and V. Jankauskas, *J. Phys. Chem. C*, 2012, **116**, 15878–15887.

27 T. Malinauskas, M. Daskeviciene, G. Bubniene, I. Petrikyte, S. Raisys, K. Kazlauskas, V. Gaidelis, V. Jankauskas, R. Maldzius, S. Jursenas and V. Getautis, *Chem. Eur. J.*, 2013, **19**, 15044–15056.

28 L. Minuti, A. Taticchi, E. Gacs-Baitz and A. Marrocchi, *Tetrahedron*, 1995, **51**, 8953–8958.

29 H. E. Zimmerman and V. Suryanarayan, *Eur. J. Org. Chem.*, 2007, **2007**, 4091–4102.

30 S. Zheng, H. Tan, X. Zhang, C. Yu and Z. Shen, *Tetrahedron Lett.*, 2014, **55**, 975–978.

31 M. Orchin and R. A. Friedel, *J. Am. Chem. Soc.*, 1949, **71**, 3002–3005.

32 P. M. G. Bavin, *Can. J. Chem.*, 1960, **38**, 1148–1153.

33 Y. Song, W. Xu and D. Zhu, *Tetrahedron Lett.*, 2010, **51**, 4894–4897.

34 A. Buckley, Ed., *Organic light-emitting diodes (OLEDs): materials, devices and applications*, Woodhead Publishing, Oxford ; Philadelphia, 2013.

35 M. J. Frisch, G. W. Trucks, H. B. Schlegel, G. E. Scuseria, M. A. Robb, et. al, GAUSSIAN 09 (Revision D. 01), Gaussian, Inc., Wallingford, CT, USA, 2009.

36 A. Tomkeviciene, J. V. Grazulevicius, K. Kazlauskas, A. Gruodis, S. Jursenas, T.-H. Ke and C.-C. Wu, *J. Phys. Chem. C*, 2011, **115**, 4887–4897.

37 F. B. Dias, K. N. Bourdakos, V. Jankus, K. C. Moss, K. T. Kamtekar, V. Bhalla, J. Santos, M. R. Bryce and A. P. Monkman, *Adv. Mater.*, 2013, **25**, 3707–3714.

38 A. Tomkeviciene, G. Puckyte, J. V. Grazulevicius, K. Kazlauskas, S. Jursenas and V. Jankauskas, *Dyes and Pigments*, 2013, **96**, 574–580.

39 A. Köhler and H. Bässler, *Mat. Sci. Eng. R*, 2009, **66**, 71–109.

40 M. Ramart-Lucas, M. J. Matti and T. Guilmart, *Bull. Soc. Chim. Fr.*, 1948, **15**, 1215–1225.

41 Y. Sun, N. C. Giebink, H. Kanno, B. Ma, M. E. Thompson and S. R. Forrest, *Nature*, 2006, **440**, 908–912.

42 R. Kersting, B. Mollay, M. Rusch, J. Wenisch, G. Leising and H. F. Kauffmann, *J. Chem. Phys.*, 1997, **106**, 2850–2864.

43 R. Karpicz, S. Puzinas, S. Krotkus, K. Kazlauskas, S. Jursenas, J. V. Grazulevicius, S. Grigalevicius and V. Gulbinas, *J. Chem. Phys.*, 2011, **134**, 204508–204516.

44 M. Cekaviciute, J. Simokaitiene, V. Jankauskas, S. Raisys, K. Kazlauskas, S. Jursenas and J. V. Grazulevicius, *J. Phys. Chem. C*, 2013, **117**, 7973–7980.

45 S. Raisys, K. Kazlauskas, M. Daskeviciene, T. Malinauskas, V. Getautis and S. Jursenas, *J. Mater. Chem. C*, 2014, **2**, 4792–4798.

46 T. Aimono, Y. Kawamura, K. Goushi, H. Yamamoto, H. Sasabe and C. Adachi, *Appl. Phys. Lett.*, 2005, **86**, 071110.

47 H.-H. Fang, J. Yang, J. Feng, T. Yamao, S. Hotta and H.-B. Sun, *Laser Photonics Rev.*, 2014, **8**, 687–715.

48 J. Chen, C. C. W. Law, J. W. Y. Lam, Y. Dong, S. M. F. Lo, I. D. Williams, D. Zhu and B. Z. Tang, *Chem. Mater.*, 2003, **15**, 1535–1546.

49 K. Kazlauskas, G. Kreiza, E. Arbačiauskienė, A. Bieliauskas, V. Getautis, A. Šačkus and S. Juršėnas, *J. Phys. Chem. C*, 2014, **118**, 25261–25271.

50 A. Miasojedovas, K. Kazlauskas, G. Armonaite, V. Sivamurugan, S. Valiyaveettil, J. V. Grazulevicius and S. Jursenas, *Dyes Pigm.*, 2012, **92**, 1285–1291.

51 T. Serevičius, R. Komskis, P. Adomėnas, O. Adomėnienė, V. Jankauskas, A. Gruodis, K. Kazlauskas and S. Juršėnas, *Phys. Chem. Chem. Phys.*, 2014, **16**, 7089–7101.

52 C. M. Heller, I. H. Campbell, B. K. Laurich, D. L. Smith, D. D. C. Bradley, P. L. Burn, J. P. Ferraris and K. Müllen, *Phys. Rev. B*, 1996, **54**, 5516–5522.

53 R. Jakubiak, C. J. Collison, W. C. Wan, L. J. Rothberg and B. R. Hsieh, *J. Phys. Chem. A*, 1999, **103**, 2394–2398.

54 M. A. Díaz-García, E. M. Calzado, J. M. Villalvilla, P. G. Boj, J. A. Quintana, F. Giacalone, J. L. Segura and N. Martín, *J. Appl. Phys.*, 2005, **97**, 063522.

55 E. M. Calzado, J. M. Villalvilla, P. G. Boj, J. A. Quintana and M. A. Díaz-García, *Org. Electron.*, 2006, **7**, 319–329.

56 A. Camposeo, E. Mele, L. Persano, D. Pisignano and R. Cingolani, *Phys. Rev. B*, 2006, **73**, 165201.

57 E. M. Calzado, J. M. Villalvilla, P. G. Boj, J. A. Quintana, R. Gomez, J. L. Segura and M. A. Diaz-Garcia, *J. Phys. Chem. C*, 2007, **111**, 13595–13605.

58 B. H. Wallikewitz, D. Hertel and K. Meerholz, *Chem. Mater.*, 2009, **21**, 2912–2919.

59 G. Tsiminis, Y. Wang, P. E. Shaw, A. L. Kanibolotsky, I. F. Perepichka, M. D. Dawson, P. J. Skabara, G. A. Turnbull and I. D. W. Samuel, *Appl. Phys. Lett.*, 2009, **94**, 243304.

60 E. Y. Choi, L. Mazur, L. Mager, M. Gwon, D. Pitrat, J. C. Mulatier, C. Monnereau, A. Fort, A. J. Attias, K. Dorkenoo, J. E. Kwon, Y. Xiao, K. Matczyszyn, M. Samoc, D.-W. Kim, A. Nakao, B. Heinrich, D. Hashizume, M. Uchiyama, S. Y. Park, F. Mathevet, T. Aoyama, C. Andraud, J. W. Wu, A. Barsella and J. C. Ribierre, *Phys. Chem. Chem. Phys.*, 2014, **16**, 16941.

61 J. C. Ribierre, G. Tsiminis, S. Richardson, G. A. Turnbull, I. D. W. Samuel, H. S. Barcena and P. L. Burn, *Appl. Phys. Lett.*, 2007, **91**, 081108.

62 G. Heliotis, D. D. C. Bradley, G. A. Turnbull and I. D. W. Samuel, *Appl. Phys. Lett.*, 2002, **81**, 415–417.

63 C. Gadermaier, L. Romaner, T. Piok, E. J. W. List, B. Souharce, U. Scherf, G. Cerullo and G. Lanzani, *Phys. Rev. B*, 2005, **72**, 045208.

64 E. M. Calzado, P. G. Boj and M. A. Díaz-García, *Int. J. Mol. Sci.*, 2010, **11**, 2546–2565.

65 H. Bässler, *phys. stat. sol. (b)*, 1993, **175**, 15–56.